Utilization of Complexity to Quantify the Regularity and Stochasticity of Nanocrystal Structure

Q. Guo, B. Song, F. Xie, M. Xie and X. Jiao*

National Synchrotron Radiation Laboratory, University of Science and Technology of China, Hefei, Anhui 230029, P.R. China

Received: 25.10.2024 & Accepted: 14.03.2025

Doi: 10.12693/APhysPolA.147.422 *e-mail: xjiao@ustc.edu.cn

Unlike conventional materials, which express functionalities by chemical compositions, nanocrystals generate and manipulate their functionalities by hierarchical structures. Considering optoelectronics, it is believed that materials with more regular structural arrangements have a stronger potential for better performance, while the stochastic structure deteriorates performance by dissipating energy flow through irregularity. People have therefore put much effort into characterizing structural regularity and stochasticity for better establishment of structure-functionality correlations. Conventionally, multiple advanced techniques are used collectively to explore structural details, such as electron microscopy for morphology, X-ray diffraction for crystallinity, and X-ray scattering for domain structures. With fortunate achievement of rich structural information, we, as physicists, ask whether a single and simple parameter can be provided to quantify the structural regularity and stochasticity. Based on renormalization group theory, structures are formed by competing long-range and short-range interactions; thus, features across a wide range of scales are correlated. There is a hidden link between structures across different scales, which can be quantified by exploring the overlaps between different renormalization group layers. This type of quantification is embodied in the concept of complexity. Its value corresponds to the extent to which a given structure differs from itself across varying length scales. With it, we successfully quantify the structural complexity of nanocrystals hierarchically, and it corresponds positively to the regularity and stochasticity characterized by other methods. And the trend of complexity obtained by the novel method correlates well with device performance. Namely, higher complexity corresponds to deteriorated device performance.

topics: complexity, renormalization group (RG), nanocrystals, stochasticity

1. Introduction

Even a single image possesses a tremendous amount of information. From the perspective of statistics, an 8-bit gray image with 512×512 pixels is a collection of 262144 individual pixels, each of which randomly displays a value ranging from 0 to 255. Thus, an image can be considered an ensemble of random variables with certain probabilistic properties determined by the measured gray scale histograms [1, 2]. In the context of pictorial representation of data, pixels at different locations are correlated, and the whole image incorporates a tremendous amount of structural details across a wide range of scales. Taking the crystal as a specific example, it includes many structural details, such as phase separation domain size, domain shape, crystallite orientation, crystallinity, etc. [3–5]. From a perceptive intuition perspective, images with wider variation of structural details and richer collection of structural features are considered to be more "complex". Thus, it should be possible for an analytical concept of complexity to be extracted from images and used to compare structures quantitatively [6, 7]. According to previous studies, the concept of complexity has been frequently applied to compare the structures of natural patterns [8], artistic workpieces [6, 9, 10], and even human faces [11]. In addition, the significance of the concept of complexity in the research of microstructures and morphology is widely acknowledged [12–15]. Intuitively, people frequently remark that scientific images with higher complexity indicate stronger irregularity and stochasticity of microstructures. Such irregularities further deteriorate the device performance of materials [16].

However, the quantitative analysis of complexity regarding scientific images is relatively sparse, based on our humble observation. Looking closely into certain scientific research fields, such as organic solar cells or perovskite optoelectronics [17–20], nearly all publications contain some scientific images characterizing the structural features of samples of interest. However, many of these images were published as intuitive representations of structural

properties without their quantitative analysis. This leads to an awkwardness: although clear comparisons with robust guidelines can be acquired for images with different features (i.e., amorphous vs crystalline), only qualitative comparisons with vague remarks are usually presented for images with similar features (i.e., samples with similar levels of crystallinity). For instance, we summarize some microstructural images taken previously, which are shown in Fig. S1 in the supplementary information [21]. Although we can unambiguously point out that materials at various volume ratios form different structural characteristics (PBDB-T/ITIC films with 0% 1,8-diiodooctane (DIO), 0.5% DIO, and 1% DIO), it is hard for us to quantify them further. To this end, many non-specialized ordinary words (I humbly believe these should not be used in scientific publications), such as "look like", "resemble", etc., are used. This makes it difficult to conduct comparisons between structures with similar, though not entirely identical, features.

A well-known concept related to "complex" structure is hierarchy. Unlike the traditional view in solid physics, where the structures are comprised of lattice space across all length scales, the hierarchical perspective assumes that different spatial features exist across multiple length scales. For instance, in the study of nanocrystals, it is not enough to only consider the crystal size and shape. Instead, we must take comprehensive consideration regarding size, shape, orientation of crystals, and even the space between them. Information is not located at a single length scale, requiring the joint application of many characterization tools [22–24]. The canonical way of covering these multi-scale parameters requires many independent measurements and experiments. For instance, electron microscopy is used to observe crystallite size and shape [25], X-ray diffraction is used to quantify the crystallinity [26], grazing-incidence wide-angle X-ray scattering is used to determine the crystallite orientation [27], small-angle X-ray scattering is used to monitor the polydispersity index of size distribution [28]. We remark that the structural parameters across a wide range of length scales probed by the above techniques are correlated hierarchically [29]. Although a given technique only provides "apparent" sensitivity to a limited length scale, hidden structural information spanning other length scales can be inferred by in-depth analysis. A telling observation lies in electron microscopy images of nanocrystals. Even though the "apparent" structural features depicted by the electron microscope are the morphology of nanocrystals (size and shape of nanocrystals), other smaller-scale structural details (crystalline ordering and orientation) can still be inferred with careful analysis. Herein, the linkage between structural features across different scales is addressed by complexity. Higher value indicates greater difference across varying length scales.

In this manuscript, we utilized a multi-scale method to analyze the complexity of scanning electron microscope (SEM) images with similar appearances. It is conducive to compare, differentiate, and analyze seemingly similar structures. With the aid of the renormalization group (RG) transformation, we were able to not only extract the total complexity of the whole image but also quantify the partial complexity at each coarse-graining scale. This enables the approach to identify the specific length scale with dominant complexity [8, 30]. In addition, we established a connection between this value and other measurements, such as the scattering measurements.

2. Methods

Inspired by RG theory, a multistep coarse-graining method by computing the overlap between neighboring RG layers was utilized to quantify the complexity of SEM images. Unlike other methods based on Fourier transformation [31, 32], image entropy [33], or correlation functions [34], this method directly probes the similarity between neighboring length scales by coarse-graining. Our intuitive perception of complexity is as follows: a system with a low level of complexity should possess similar characteristic structures at different scales, while a system with a high level of complexity should exhibit different structures across different scales. Taking the salt NaCl as an example, it adopts a cubic unit cell at the nanoscale and similarly exhibits a cubic shape at the macroscale. Although the structures at the nanoscale and macroscale are observed by distinctly different equipment (e.g., X-ray diffraction for nanoscale and optical microscopy for macroscale), the similarity of the images taken at the nanoscale and macroscale is obvious [35]. This type of self-similarity is inversely correlated with structural complexity. In other words, if the shape of the unit cell at the nanoscale is known, it can be anticipated that the macroscopic crystals will also be formed with the same shape.

Based on the above intuitive perception, a quantitative definition of structural complexity is given. Any image can be described by a function $f(\boldsymbol{x})$, where $\boldsymbol{x}$ is a position vector, corresponding to the image pixels, and $f(\cdot)$ is the gray-scale intensity. For such an image, the RG transformation is applied, and successively coarse-graining patterns are generated. In this way, the structural complexity is calculated as follows,

$$C_k = \left| \langle f_k^x | f_{k+\mathrm{d}k}^x \rangle - \frac{1}{2} \Big(\langle f_k^x | f_k^x \rangle + \langle f_{k+\mathrm{d}k}^x | f_{k+\mathrm{d}k}^x \rangle \Big) \right|, \tag{1}$$

where $\langle f^x | g^x \rangle$ calculates the overlap of two images described by $f(\boldsymbol{x})$ and $g(\boldsymbol{x})$, and k represents the scale. Note that "overlap" herein does not denote the

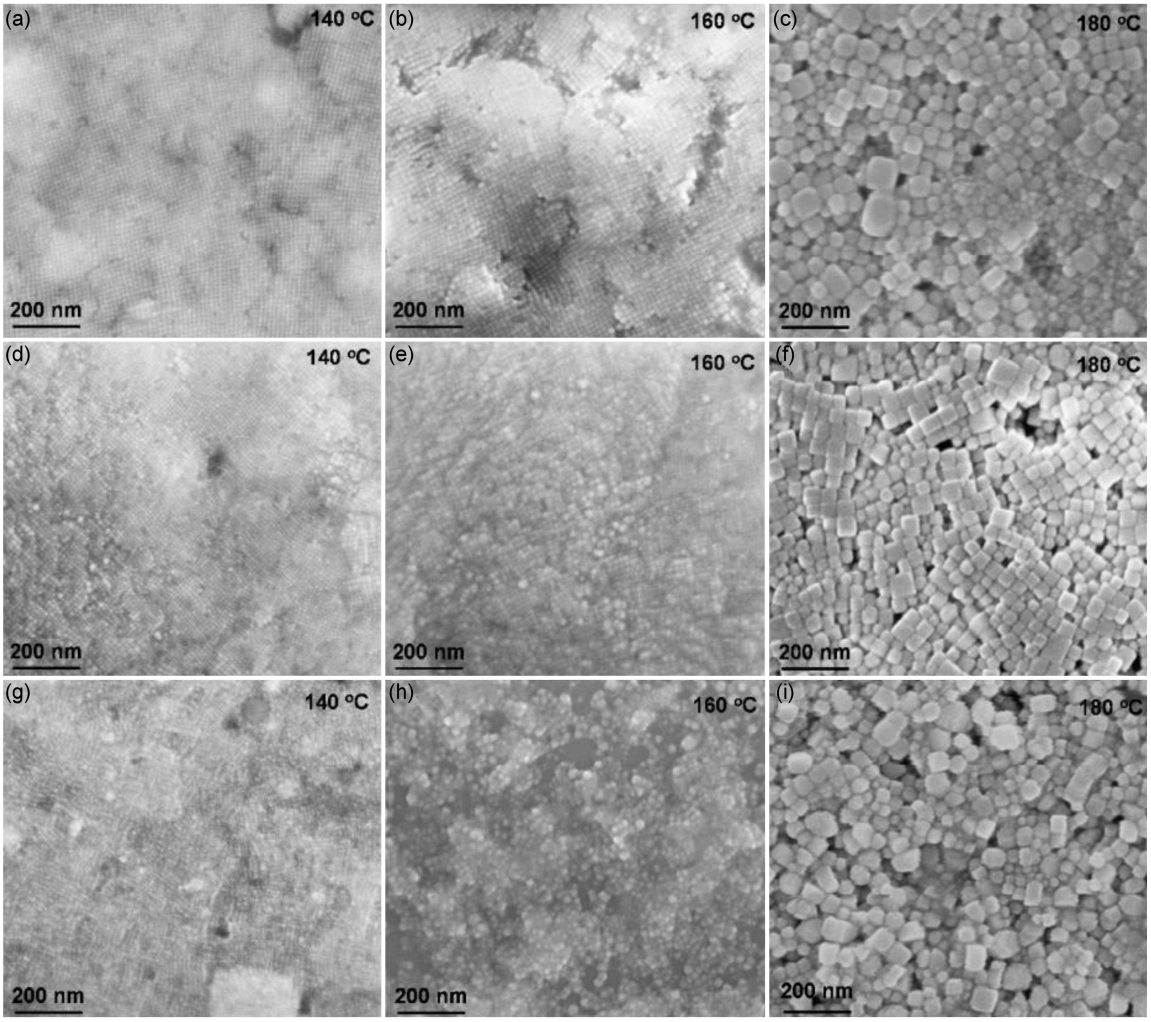

Fig. 1. (a–c) Field emission scanning electron microscopy (FE-SEM) images of (a–c) $CsPbBr_3$, (d–f) $CsPbBr_xI_{3-x}$, (g–i) $CsPbBr_xCl_{3-x}$ at different temperatures [36]. Reproduced with permission from [36]. Copyright 2017 American Chemical Society.

pictorial meaning of overlap among two structures, but rather a mathematical notion depicting the similarity between $f(\boldsymbol{x})$ and $g(\boldsymbol{x})$. The calculation of $\langle f^x|g^x\rangle$ is simply the sum of the elements in the matrix obtained from the Hadamard product of two matrices representing $f(\boldsymbol{x})$ and $g(\boldsymbol{x})$. In this context, the Hadamard product involves element-wise multiplication of the two matrices, followed by summing all the resulting elements to compute the final value $\langle f^x|g^x\rangle$. The subscripts of f_k^x and $f_{k+\mathrm{d}k}^x$ represent the coarse-graining scale of RG layers, so f_k^x means the image used the multistep coarse-graining method at RG layers $= k$ (the coarse-graining scale $= 2^{k+1}$). It is natural that C_k is the quantification of the overlap between a coarse-grained pattern $f_k(\boldsymbol{x})$ and a bit coarser version $f_{k+\mathrm{d}k}(\boldsymbol{x})$. Specifically, a value of $C_k = 0$ indicates that coarse-graining does not cause spatial variation between $f_k(\boldsymbol{x})$ and $f_{k+\mathrm{d}k}(\boldsymbol{x})$. On the contrary, a value of $C_k > 0$ suggests that the structures under different levels of coarse-graining are different and may contribute to complexity. Summing up the C_k over all scales, a multiscale structural complexity C can be obtained,

$$C = \sum_k C_k. \tag{2}$$

3. Results

Considering that we do not have adequate expertise in terms of fabrication and characterization of nanocrystals, we decided to borrow published data from prestigious journals. In this manuscript, all of the SEM images and X-ray scattering images are quoted from an article published by some influential scholars in the Journal of Physical Chemistry Letters [35]. Figure 1 is a collection of SEM images of a series of perovskite nanocrystals, including $CsPbBr_3$, $CsPbBr_xI_{3-x}$, and $CsPbBr_xCl_{3-x}$. This figure forms a well-organized matrix for comparison: along the column direction, perovskite

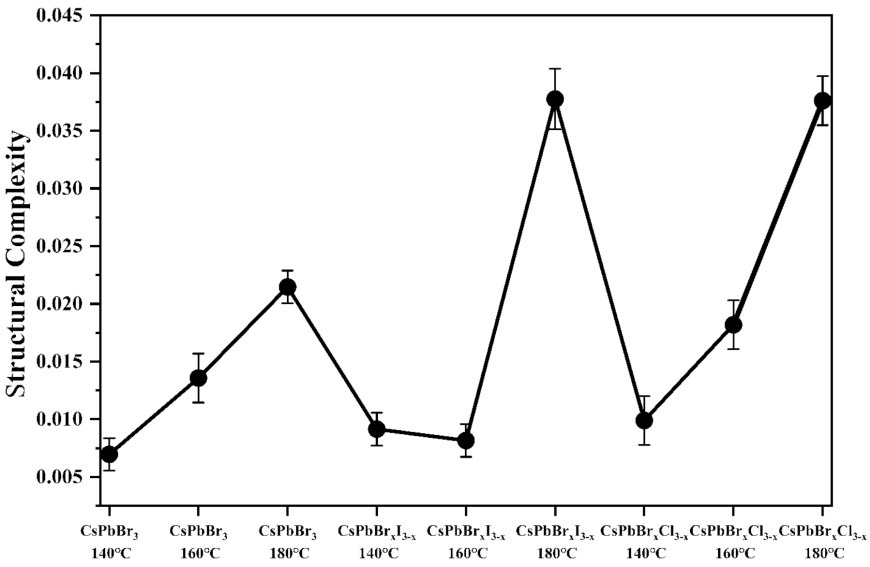

Fig. 2. Structural complexity of $CsPbBr_3$, $CsPbBr_xI_{3-x}$, and $CsPbBr_xCl_{3-x}$ at 140°C, 160°C, and 180°C, respectively.

nanocrystals of all components are thermally annealed at successively increasing temperatures of 140°C (Fig. 1a, d, g), 160°C (Fig. 1b, e, h), and 180°C (Fig. 1c, f, i); along the row direction, perovskite nanocrystals annealed at all temperatures have different compositions, denoted as $CsPbBr_3$ (Fig. 1a, b, c), $CsPbBr_xI_{3-x}$ (Fig. 1d, e, f), and $CsPbBr_xCl_{3-x}$ (Fig. 1g, h, i). Visual inspection of Fig. 1 reveals that although the morphology of all compositions annealed at different temperatures can be easily differentiated along the row direction, the differences among samples with different compositions annealed at the identical temperature are difficult to define or measure. More specifically, although we can say that the three samples — $CsPbBr_3$, $CsPbBr_xI_{3-x}$, and $CsPbBr_xCl_{3-x}$ — produce crystals progressively larger in size and sharper in shape, it is hard to tell the quantitative difference between these samples annealed at identical temperature as a function of composition. This type of confusion about how to compare structures with similar features makes us wonder whether there is any parameter that can be used for a more quantitative analysis or not. We resort to the concept of complexity with the aim of structural quantification. Herein, we utilize the above-devised multi-length scale complexity measure to analyze the SEM images and try to establish a quantitative comparison.

Figure 1 presents a collection of SEM images of nanocrystals. People often rely on human cognitive abilities to conclude that the structures in Fig.1c, f, i are more complex than those in Fig. 1a, d, g. This type of observation is on the subjective side and only helps to make a qualitative comparison: (i) the nanocrystals in Fig. 1c, f, i are characterized by a broader range of size distributions; (ii) the shape of nanocrystals in Fig. 1c, f, i changes more obviously. Although this conclusion is straightforward and correct, no quantitative comparison has been made, such as how much more "complex" the structures in Fig. 1c, f, i are than those in Fig. 1a, d, g. To address this, we need to find a robust definition of complexity, which should formulate the following requirements: (i) it should aggregate information about different length scales; (ii) it should be analytically defined, rather than relying on subjective intuition; (iii) it must provide numerical results, capable of distinguishing closely similar structures. Thus, structural complexity is calculated based on the technique introduced in Sect. 2.

Figure 2 plots the structural complexity of different images from Fig. 1. It is noteworthy that for all three compositions, the samples annealed at 180°C exhibit significantly higher structural complexity than their counterparts annealed at lower temperatures. This seems surprising in the sense that if the structural complexity is the highest for 180°C, the corresponding regularity should be the lowest. However, this would contradict the observation that samples processed at 180°C exhibit well-defined crystal morphology and significantly larger crystal sizes compared to those processed at lower temperatures. This seemingly contradictory conclusion is reasonable, as structural complexity is a comprehensive concept that accounts for structural irregularities across multiple length scales. Although the samples annealed at 180°C exhibit sharper morphologies and well-defined crystal sizes, suggesting a higher degree of regularity, they also possess crystal boundaries and polydispersity, which conversely enhances the overall complexity. More insights will be given in Sect. 4.

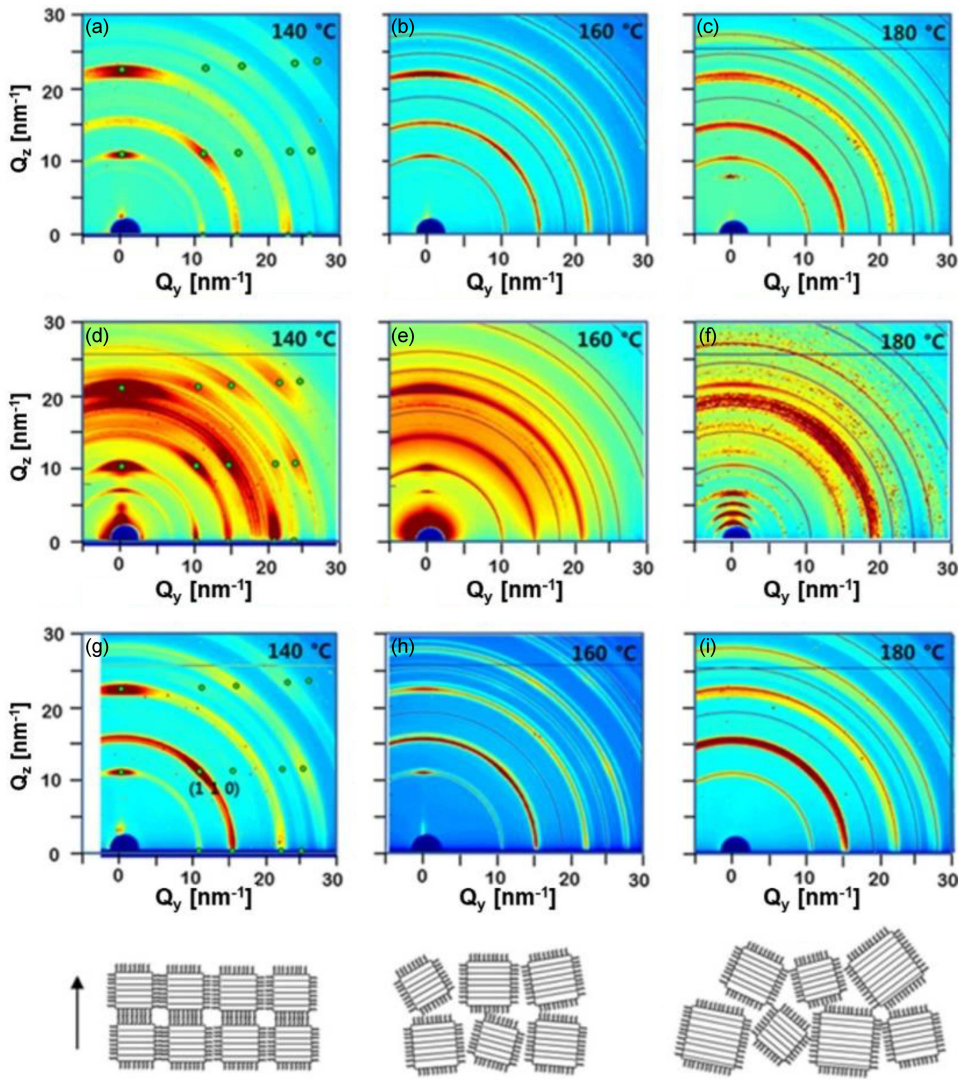

Fig. 3. Grazing-incidence wide-angle X-ray scattering (GIWAXS) images measured from self-assemblies of spin-coated (a–c) $CsPbBr_3$, (d–f) $CsPbBr_xI_{3-x}$, and (g–i) $CsPbBr_xCl_{3-x}$ nanocrystals synthesized at different reaction temperatures [36]. Reproduced with permission from [36]. Copyright 2017 American Chemical Society.

To make things more interesting, the value of complexity is not only correlated with the SEM images, but also with the structural information obtained by other complementary techniques. According to the original literature, the authors also investigated these samples using X-ray scattering and diffraction methods, where the former describes the mesoscale structure and the latter depicts the nanoscale structure. Herein, we further explore its connection with the scattering method. By utilizing grazing-incidence wide-angle X-ray scattering (GIWAXS), it is found that the nanocrystals in samples annealed at higher temperatures arrange themselves in a more randomly oriented way. As seen in the last column in Fig. 3, 180°C samples all display diffraction rings without much preferential orientation, whereas stronger orientation preferences are observed at lower temperatures. In addition to intuitive perception, the calculated structural complexity derived from the SEM image is consistent with GIWAXS results, where 180°C samples exhibit significantly higher complexity than those annealed at lower temperatures. This consistency between complexity from SEM images and GIWAXS observations further proves the applicability of this novel idea of structural complexity in the understanding of structures.

The comparison of structural complexity presented above is conducted on the whole image without distinguishing the length scale dependence. Considering that the numerical calculation of complexity is based on the renormalization group (RG) transformation between coarse-grained images, the value of partial complexity of each RG layer also provides meaningful implications about the contribution to the overall complexity from each individual length scale (see (1)). In other words, it is possible to identify which level of coarse-grained images

dominates the overall structural complexity by evaluating the partial complexity at each level of length scale. In practice, if the plot of C_k vs k is drawn, people should be able to tell which length scale is the one with the most complexity by finding the maximum of C_k. By definition, the characteristic length scale corresponding to the k-th step with maximum C_k is the length scale at which the image possesses the most dominant structural features.

To prove the above idea, the relationships between C_k and k are plotted and displayed in Fig. 4. Looking closely at the sample of $CsPbBr_3$ at different temperatures, it is found that the sample annealed at 180°C shows the maximum at $k = 4$, while its counterpart annealed at 140°C shows the maximum at $k = 2$. This indicates that $CsPbBr_3$ annealed at 140°C exhibits the dominant structural features at a length scale of 8.464 nm, while the dominant features increase in size to 33.856 nm at 180°C. The actual length scale value above is converted from the coarse-graining scale at k by the relation according to which the length scale is equal to the coarse-graining scale (2^{k+1}) times the length of one pixel. For example, if the coarse-graining scale equals 8 at $k = 2$, the length scale is 8.464 nm (8 pixel ×1.058 nm/pixel), where 1.058 nm/pixel is the calibration standard for the SEM image. Besides, to further prove the suitability of this novel method, we compared the dominant structural scale obtained with power spectral density (PSD) calculated by the Fourier transformation and used the Lorentz correction method to accurately determine the peak position of PSD. As seen in Fig. S2 in supplementary information [21], the dominant structural scales identified by PSD are 12.5 nm and 44.8 nm (calculated by $d = \frac{2\pi}{q}$), consistent with the results from structural complexity. Note that there exists a 20–30% offset toward shorter length due to the fact that the partial complexity method generates discrete values without enough resolution. The same trend can be observed for samples with other compositions. Note that $CsPbBr_3$ at 160°C exhibits bizarre behavior, where complexity suddenly increases at $k = 6$ due to the impact of large cracking features.

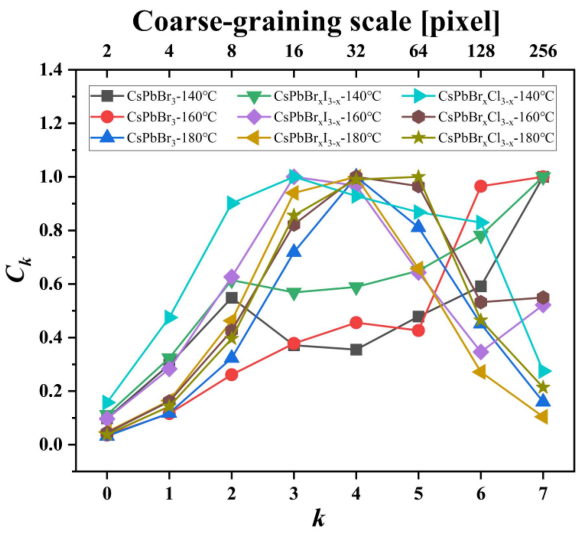

Fig. 4. Partial complexity C_k of different samples on RG transformation step k. The value of C_k is normalized to unity for easier comparison. Uncertainty is less than 10%.

4. Discussion

With the preceding investigation and discussion, it becomes clear that structural complexity can serve as a sensitive probe for quantifying the regularity and stochasticity of nanocrystals. With its aid, superficial perceptive intuition can be corrected, and structural information from different tools can be bridged. Inspired by the above study regarding nanocrystal SEM data, we humbly believe that structural complexity is a more general approach to quantifying irregularity than crystallinity, since the latter tends to focus on the local situation of each crystal, without much account for the space among them. These parameters, including crystal size, size polydispersity, and crystal shapes, are all interrelated with structural complexity and significantly influence its value. Intuitively, samples with wider size polydispersity and wider shape variation are considered more "complex". Also, with the analysis of partial structural complexity as a function of length scale, the degree of contribution to the total complexity from each individual length scale can also be delineated, and a clearer picture regarding hierarchical structure can be obtained. The hierarchical structure changes at different coarse-graining scales are shown in Figs. S3 and S4 of the supplementary information [21].

It should be recognized that the structural complexity discussed in this manuscript is not the only type of complexity. Besides structural complexity, we extend our investigation toward entropic complexity and Kolmogorov complexity, which have intrinsic connections, but with a clear difference. Simply put, entropic complexity utilizes Shannon entropy to calculate the value of complexity and characterizes the degree of randomness rather than irregularity [7, 37]. If you do not understand the difference between randomness and irregularity, imagine the case of white noise. A picture of white noise possesses the highest level of entropic complexity but with the lowest structural complexity, suggesting the most random but at the same time regular structure (i.e., any localized areas show the same level of randomness). With this achievement, we move further to test whether other types of complexity as a function of length scale can also generate inspiring information about regularity and stochasticity in the hope of bringing a novel

TABLE I

Structural complexity, entropic complexity, and compression ratio of different samples.

Parameter	$CsPbBr_3$			$CsPbBr_xI_{3-x}$			$CsPbBr_xCl_{3-x}$		
	Fig. 1a	Fig. 1b	Fig. 1c	Fig. 1d	Fig. 1e	Fig. 1f	Fig. 1g	Fig. 1h	Fig. 1i
	−140°C	−160°C	−180°C	−140°C	−160°C	−180°C	−140°C	−160°C	−180°C
structure complexity	0.00696	0.01357	0.02147	0.00914	0.00816	0.03775	0.00989	0.01818	0.0376
entropic complexity	6.2439	7.4599	6.6767	6.6881	6.3810	7.3347	6.5370	6.3935	7.0344
compression ratio	0.5911	0.5857	0.5387	0.6032	0.5633	0.6539	0.6298	0.5229	0.5732

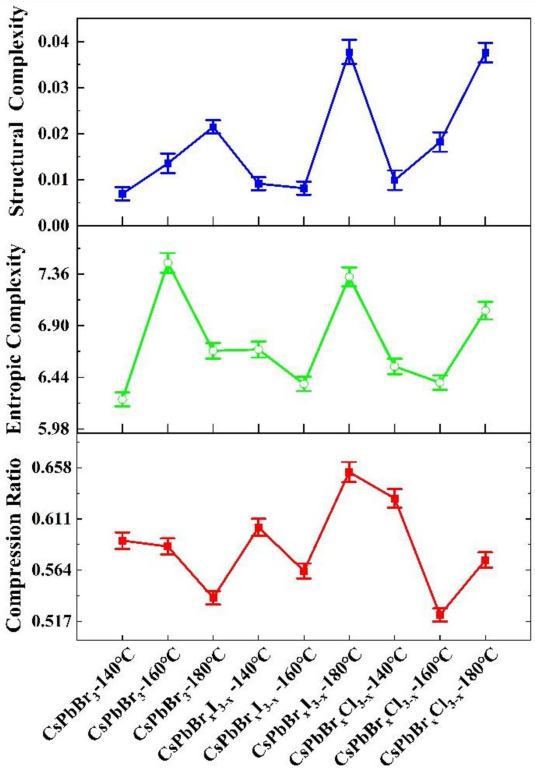

Fig. 5. Comparison of structural complexity, entropic complexity, and compression ratio of different samples.

perspective for researchers investigating multi-length scale phenomena. Before diving into this endeavor, we have to realize that there exist many definitions of complexity, most of which have a common weakness: the intuitive feeling of "complex" versus "simple" is a subjective decision made by humans, and many definitions are based on qualitative description, rather than quantitative equation. To this end, we decided to explore only entropic complexity and Kolmogorov complexity, since these two can be defined by tidy equations and quantified numerically without "observer-dependence". Entropic complexity was initially quantified by Shannon and thereafter called Shannon entropy as an alternative name [7, 37]. The mathematical definition is

$$H = -\sum_x p_x \log_2(p_x), \tag{3}$$

where p_x is the probability distribution of pixel intensity x in the investigated image. The resultant entropic complexity of all images from Fig. 1 is summarized in Table I.

It should be acknowledged that the maximum of entropic complexity occurs for a system with equal numerical distribution of each pixel intensity, namely white noise, and the value reaches 8 [38]. Table I shows that the measured entropic complexity values for the images in Fig. 1 range from 6.2 to 7.5, implying that the structures investigated in our study are not random but have detectable features. Kolmogorov complexity is defined as the length of the shortest computer program that outputs the information depicting the given structure [14]. This concept is usually difficult to quantify, but the calculation becomes practical for images. Herein, we utilized the compression ratio to inversely represent Kolmogorov complexity, defined as the file size of the compressed image divided by the size of the original file, using the LZMA2 compression method [39]. The compression ratio is obtained and also tabulated in Table I. It should be mentioned that white noise is characterized as a value of 1 in terms of Kolmogorov complexity due to the fact that no spatial correlation can be established and therefore no meaningful compression algorithm can take effect. For comparison, the resultant values in our study span from 0.52 to 0.66, i.e., are considerably lower than 1. This clearly indicates that the structures of samples in Fig. 1 are far from being random because of certain regularity, thus making the compression algorithm effective. To be clearer, the comparisons of all three complexity measures are summarized and plotted in Fig. 5. An evident correlation can be seen between structural complexity and entropic complexity. On the other hand, the trend of Kolmogorov complexity evolves in quite a different manner. This observation definitely indicates that structural and entropic complexities are more physically correlated than Kolmogorov complexity.

The above discussions about entropic and Kolmogorov complexity are only applied to the original images without RG transformation, thereby delivering no information regarding hierarchy. We further calculated the entropic and Kolmogorov complexity as a function of the RG layer using the coarse-graining method. It has been found that the

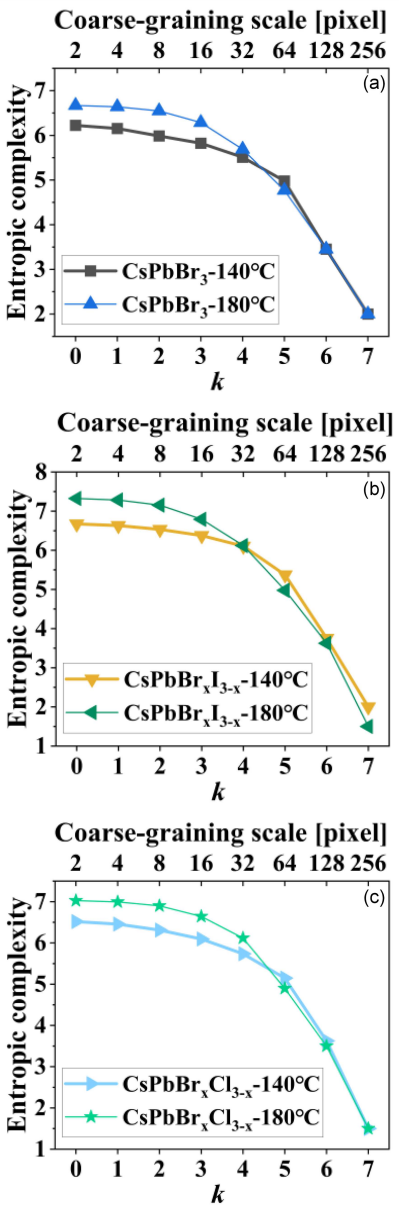

Fig. 6. Variation of entropic complexity of three samples with the coarse-graining scales at 140°C and 180°C: (a) $CsPbBr_3$, (b) $CsPbBr_xI_{3-x}$, and (c) $CsPbBr_xCl_{3-x}$. Uncertainty is less than 8%.

Kolmogorov complexity of all images rapidly reduces as a function of the RG layer, leaving the straightforward comparison of Kolmogorov complexity at transformed layers impossible (see supplementary information [21] for detailed data in Table S1). Therefore, we only focus on RG layer dependence of entropic complexity in the main text. Figure 6a, b, and c delineate the trends of entropic complexity as a function of coarse-graining scale for $CsPbBr_3$, $CsPbBr_xI_{3-x}$, and $CsPbBr_xCl_{3-x}$, respectively. Clearly, the samples annealed at 180°C exhibit a significantly faster decay rate than those annealed at 140°C. This observation indicates that the 180°C samples are more "complex" than others due to the fact that they are less similar to themselves across multiple length scales, which is consistent with the conclusion drawn from structural complexity.

Partial entropic complexity exhibits the same trend with the increase in coarse-graining scale, which means that although the sample comparison is possible, the coarse-graining-dependent entropic complexity is rendered incapable of delineating spatial correlation among samples. On the other hand, Kolmogorov complexity is similar to entropic complexity, but with a comprehensive consideration of both intensity and spatial correlation. Kolmogorov complexity in our manuscript is calculated based on a compression algorithm that looks for redundant intensity modes and repeating spatial patterns. This enables Kolmogorov complexity to quantify the state of regularity and stochasticity of both natural scenes and man-made structures. A typical example is crystal and glass. The well-arranged structure of the crystal is quite ordered and delivers a lower compression ratio, equal to 0.005729. In contrast, the randomly arranged structure of glass does not leave much convenience for the algorithm to carry on effective compression, and the compression ratio is equal to 0.026852 (see Fig. S5 in supplementary information [21]).

5. Conclusions

This manuscript stresses that regularity and stochasticity are important parameters for understanding the microstructure of nanomaterials. The extent of stochasticity is quantified by the value of structural complexity. With the discovery of structural complexity, we achieve the goal of understanding the intuitive perception of "complex" and "simple" in a quantitative manner. We are now able to explore the connection between different length scales with the help of the RG layering method, even without the knowledge of the driving force forming hierarchy. Another benefit of structural complexity originates from partial structural complexity, which allows us to distinguish which length scale is the major contributor to the total structural complexity. With its aid, we can successfully pinpoint the dominant length scale, which is beneficial for comprehending the structure of the material. In addition, the entropic complexity and Kolmogorov complexity are compared with the structural complexity. Through the examples in this manuscript, it is suggested that entropic complexity is more relevant to structural complexity than Kolmogorov complexity. Overall, three types of complexity are foreseen to work together, helping to gain more insights regarding complex structures.

See supplementary information [21] for: (i) images of atomic force microscopy (AFM) heights of PBDB-T/ITIC films with 0% DIO, 0.5% DIO,

1% DIO, (ii) power spectral density (PSD) calculated by Fourier-transformation and Lorentz correction of PSD for sample $CsPbBr_3$ at −140°C and sample $CsPbBr_3$ at −180°C, (iii) images of the sample $CsPbBr_3$ at −140°C at the different coarse-graining scales, (iv) images of the sample $CsPbBr_3$ at −180°C at the different coarse-graining scales, (v) table of entropic complexity and compression ratio of different samples as the coarse-graining scale changes, (vi) representation of crystal structure and glass structure, partial complexity C_k and partial Kolmogorov complexity of crystal and glass as a function of coarse-graining scale.

The data that support the findings of this study are available from the corresponding author upon reasonable request.

Acknowledgments

This work is supported by Key Fund Project for Youth Innovation, Anhui Provincial Natural Science Foundation, and National Key Research and Development Program of China (YD2310002006, 2308085MA19, and 2023YFA1609800).

References

[1] J.P. Crutchfield, K. Young, *Phys. Rev. Lett.* **63**, 105 (1989).

[2] T.I. Sanders, What Is Complexity?.

[3] L. Guo, Z. Xu, X. Jiao, Q. Ruan, X. Xie, B. Xiao, Q. Li, Y. Cai, S. Liu, *ACS Appl. Energy Mater.* **4**, 10187 (2021).

[4] J. Pan, Z. Dong, B. Wang, Z. Jiang, C. Zhao, J. Wang, C. Song, Y. Zheng, C. Li, *Appl. Catal. B Environ.* **242**, 92 (2019).

[5] W.L. Tan, Y.Y. Choo, W. Huang, X. Jiao, J. Lu, Y.-B. Cheng, C.R. McNeill, *ACS Appl. Mater. Interfaces* **11**, 39930 (2019).

[6] S. Lakhal, A. Darmon, J.-P. Bouchaud, M. Benzaquen, *Phys. Rev. Res.* **2**, 022058(R) (2020).

[7] R. López-Ruiz, H.L. Mancini, X. Calbet, *Phys. Lett. A* **209**, 321 (1995).

[8] A.A. Bagrov, I.A. Iakovlev, A.A. Iliasov, M.I. Katsnelson, V.V. Mazurenko, *Proc. Natl. Acad. Sci. USA* **117**, 30241 (2020).

[9] G.-H. She, A.D.K.-T. Lam, *J. Internet Technol.* **17**, 109 (2016).

[10] A. Karjus, M. Canet Solf, T. Ohm, S.E. Ahnert, M. Schich, *EPJ Data Sci.* **12**, 21 (2023).

[11] S.R. Lehky, A.H. Phan, A. Cichocki, K. Tanaka, *Neural Comput.* **32**, 281 (2020).

[12] R.C. Alamino, *J. Phys. A Math. Theor.* **48**, 275101 (2015).

[13] D.T. Mihailović, G. Mimić, E. Nikolić-Djorić, I. Arsenić, *Open Phys.* **13**, 1 (2015).

[14] D.H. Wolpert, W. Macready, *Complexity* **12**, 77 (2007).

[15] T. Steifer, M. Lewandowski, *Biomed. Signal Process. Control* **51**, 235 (2019).

[16] H. Cho, S.-H. Jeong, M.-H. Park et al., *Science* **350**, 1222 (2015).

[17] H. Liu, Z. Chen, R. Peng et al., *Chem. Eng. J.* **474**, 145807 (2023).

[18] S. Hong, B. Park, C. Balamurugan, J. Lee, S. Kwon, *Heliyon* **9**, e18209 (2023).

[19] L. Protesescu, S. Yakunin, M.I. Bodnarchuk, F. Krieg, R. Caputo, C.H. Hendon, R.X. Yang, A. Walsh, M.V. Kovalenko, *Nano Lett.* **15**, 3692 (2015).

[20] W.S. Yang, J.H. Noh, N.J. Jeon, Y.C. Kim, S. Ryu, J. Seo, S.I. Seok, *Science* **348**, 1234 (2015).

[21] Q. Guo, B. Song, F. Xie, M. Xie, X. Jiao, *Acta Phys. Pol. A* **147**, 422.S1 (2025).

[22] I. Kriegel, F. Scotognella, *Thin Solid Films* **612**, 327 (2016).

[23] D. Liang, C. Dong, L. Cai et al., *Small* **17**, 2100972 (2021).

[24] E.L. Heeley, K. Billimoria, N. Parsons, Ł. Figiel, E.M. Keating, C.T. Cafolla, E.M. Crabb, D.J. Hughes, *Polymer* **193**, 122353 (2020).

[25] K. Kaneko, S. Matsumura, K. Ikematsu, Y. Kato, Y. Tomokiyo, A. Watanabe, T. Masumoto, *Scr. Mater.* **48**, 915 (2003).

[26] G.H. Liu, K.Y. Liu, G.Y. Zhai, J.H. Zhao, Z.G. Guo, *Mar. Pet. Geol.* **150**, 106124 (2023).

[27] P.S. Wang, Y.L. Ma, P. Yin, D.D. Cai, S. Wan, Q.D. Zheng, *Chem. Eng. J.* **418**, 129497 (2021).

[28] T. Rattanawongwiboon, S. Soontaranon, K. Hemvichian, P. Lertsarawut, S. Laksee, R. Picha, *Radiat. Phys. Chem.* **191**, 109842 (2022).

[29] R. Agneeswari, D. Kim, S.W. Park, S. Jang, H.S. Yang, I. Shin, J.H. Jeong, V. Tamilavan, Y.K. Jung, S.H. Park, *Polymer* **229**, 123991 (2021).

[30] B. Gidas, *IEEE Trans. Pattern Anal. Mach. Intell.* **11**, 164 (1989).

[31] Y. Su, Z. Wang, L. Jing, *Displays* **69**, 102060 (2021).

[32] M. Pournoury, A. Zamiri, V. Yurlov, T.Y. Kim, A. Jung, K. Oh, *Results Phys.* **14**, 102401(2019).

[33] X.L. Chen, R.M. Wang, Y.F. Cao, W.Y. Yu, J.C. Feng, *Proc. Eng.* **29**, 3959 (2012).

[34] M. Schümann, J. Morich, S. Günther, S. Odenbach, *J. Magn. Magn. Mater.* **502**, 166537 (2020).

[35] D. Mengyan, H. Biru, W. Wenjian, *J. Natl. Univ. Def. Technol.* **31**, 130 (2009).

[36] Q.V. Le, J.B. Kim, S.Y. Kim, B. Lee, D.R. Lee, *J. Phys. Chem. Lett.* **8**, 4140 (2017).

[37] S.-H. Cha, *Int. J. Math. Models Methods Appl. Sci.* **1**, 300 (2007).

[38] D.H. Zanette, *PLoS One* **13**, 0207879 (2018).

[39] C. McCarthy, LZMA2 Library, gitee.com, 2024.